



# Terahertz pulses induce segment renewal via cell proliferation and differentiation overriding the endogenous regeneration program of the earthworm *Eisenia andrei*

MAHMOUD H. ABUFADDA,<sup>1,4</sup> ANITA ERDÉLYI,<sup>2</sup> EDIT POLLÁK,<sup>2</sup>  
PRIYO S. NUGRAHA,<sup>1,3,4</sup> JÁNOS HEBLING,<sup>1,3,4</sup> JÓZSEF A.  
FÜLÖP,<sup>1,3,5</sup>  AND LÁSZLÓ MOLNÁR<sup>2,\*</sup> 

<sup>1</sup>Institute of Physics, University of Pécs, Pécs, 7624, Hungary

<sup>2</sup>Institute of Biology, University of Pécs, Pécs, 7624, Hungary

<sup>3</sup>Szentágotthai Research Centre, University of Pécs, Pécs, 7624, Hungary

<sup>4</sup>MTA-PTE High-Field Terahertz Research Group, Pécs, 7624, Hungary

<sup>5</sup>ELI-ALPS, ELI-HU Nonprofit Ltd., Szeged, 6728, Hungary

\*molnar@gamma.ttk.pte.hu

**Abstract:** Terahertz (THz) irradiation of excised *Eisenia andrei* earthworms is shown to cause overriding of the genetically determined, endogenously mediated segment renewing capacity of the model animal. Single-cycle THz pulses of 5  $\mu$ J energy, 0.30 THz mean frequency, 293 kV/cm peak electric field, and 1 kHz repetition rate stimulated the cell proliferation (indicated by the high number of mitotic cells) and both histogenesis and organogenesis, producing a significantly higher number of regenerated segments. The most conspicuous alteration in THz-treated animals was the more intense development of the new central nervous system and blood vessels. These results clearly demonstrate that THz pulses are capable to efficiently trigger biological processes and suggest potential applications in medicine.

© 2021 Optical Society of America under the terms of the [OSA Open Access Publishing Agreement](#)

## 1. Introduction

THz or far-infrared electromagnetic waves have frequencies in the 0.1–10 THz range. The investigation of the biological effects of THz radiation on biomolecules like DNA, peptides, lipids, and certain cells like fibroblasts, lymphocytes, and epidermal cells was in the focus of several studies [1], resulting in contradictory experimental results. However, there is consensus that THz waves can modify the activity of biomolecules or cells by either thermal effects or non-thermal biological effects. The former one proved to be harmful, generating cell death (apoptosis, necrosis) [2,3], or morphological injury of neurons in *in vitro* experiments [4], and expression of stress molecules (heat shock proteins, and DNA damage markers) in irradiated cells [5].

The influence of THz radiation on DNA is a debated question. No genotoxicity was found in an experiment applying pulsed, broadband THz radiation from a free-electron laser for 20 minutes [6]. In contrast, genomic instability (aneuploidy) when exposing human lymphocytes by continuous-wave THz radiation for a considerable longer time of 24 hours found by Korenstein-Ilan et al. [7]. Although the exposure time and the radiation intensity were very different in the two cases, the radiation dose was very similar, at a level of 0.1 J/cm<sup>2</sup>. In contrast to these opposite results, there is some experimental evidence on the neutral effect of THz radiation on biological systems. Applying lower-frequency (0.14 THz) pulses, no effect of THz radiation was observed on the differentiation and cell viability in cell cultures of human keratinocytes and neurons [8,9]. It was also found that THz radiation had no significant effect on the morphology, adhesion, proliferation, and differentiation of certain human cells, like epithelial and embryonic

stem cells, and on lymphocyte chromosomes in *in vitro* experiments. However, THz radiation can mediate the growth and proliferation of certain cells under certain exposure conditions [10].

Several non-thermal biological effects of 0.3–0.6 THz radiation were experimentally shown [11]. It can influence the plasma membrane permeability, resulting in either suppression or facilitation of neuronal activity [12]. Furthermore, it can accelerate cell differentiation and cellular reprogramming [13]. Based on these results, it seems that THz radiation can have a strong and versatile influence on biological systems, which sensitively depends on the irradiation parameters (spectral distribution, power, duration, electric field strength) and on the morphological and/or physiological characteristics of the biological targets.

In contrast to the *in vitro* experiments, the effects of the THz exposure at organism level were sparsely investigated. The *in vivo* biological effects of the pulsed THz radiation on mice skin wound showed that the repeated THz exposure perturbed the wound healing process which depend on cell proliferation and differentiation. The delayed wound closure was attributed to the elevated expression level of transforming growth factor-beta (TGF- $\beta$ ) signaling pathways, suggesting the importance of the understanding of the potential health hazards of THz radiation Kim et al. [14]. Because of the increasing application of THz, both in biology and medicine, it is necessary to reveal and understand its effects (either advantageous or disadvantageous) at organism level in *in vivo* experiments.

There is a relatively simple *in vivo* experimental method, used from the 18<sup>th</sup> century, the regeneration of the surgically ablated tail segments of earthworms. Earthworms have an enormous capacity to regenerate lost tail segments [15], and this process is mediated by some internal and external factors. The neural dependence of the regeneration was promulgated by Morgan [16], suggesting that certain neural factors, like neurotransmitters and neurohormones, were necessary for the formation of a regeneration blastema from which the new segments were formed. The influence of the immune system on the formation of the regeneration blastema and renewing structures was shown as well [17,18]. The effects of the internal factors on cell proliferation, differentiation, and tissue morphogenesis can be modified by certain environmental conditions, such as temperature [19], osmotic stress [20], and electromagnetic waves, like laser irradiation [21].

In this work, the effect of THz irradiation on segment regeneration kinetics of excised *Eisenia andrei* earthworms is investigated. The formation of new segments, consisting of various tissues, depends on the mitotic activity of cells, then growing and differentiation of daughter cells to specific tissue cells. However, migration of certain blast cells to the site of the injury was also observed [22,23]. The intensity of the segment formation determines the reconstruction of the original body plan of the experimental animals' characteristic for the earthworms. Both cell proliferation and growing/differentiation are genetically determined processes, which are only partially investigated and known [24]. In contrast, the segment regeneration as the consequence of molecular interactions, cellular and histological alterations can quantitatively be investigated. Therefore, the earthworm regeneration model gives a good opportunity to study the influence of the THz radiation on cells and tissues at the organism level.

The presented results show that THz pulses with well-defined parameters have beneficial effects on wound healing and segment regeneration of earthworms, suggesting that THz radiation with certain characteristics may be suitable for medical applications, too.

## 2. Materials and methods

### 2.1. Experimental animals

In all experiments healthy, sexually matured (clitellated) specimens of the earthworm *Eisenia andrei* (Annelida, Oligochaeta, Lumbricidae) were used which were handsorted from the breeding stocks maintained at standard laboratory conditions as described earlier [25]. The selected specimens were kept on wetted paper wadding for three days to remove gut content. For species

identification the mitochondrially encoded cytochrome c oxidase I (MT-CO1) gene sequestration was used [26].

## 2.2. Ablation of tail segments

A standard method developed in our laboratory was used to excise the specimens [15]. The purified animals were anaesthetized with carbonated water at 4 °C to total movelessness and insensitivity. By the aid of a stereomicroscope, 25 posteriormost segments were counted and ablated with quick, sharp scissors cutting at the segment furrow (Fig. 1). The quality of the surgical interventions (inactness of the last segment located before the cutting) was immediately inspected and only those animals were introduced into the experiments in which the segment boundary (dissepiment) was intact.

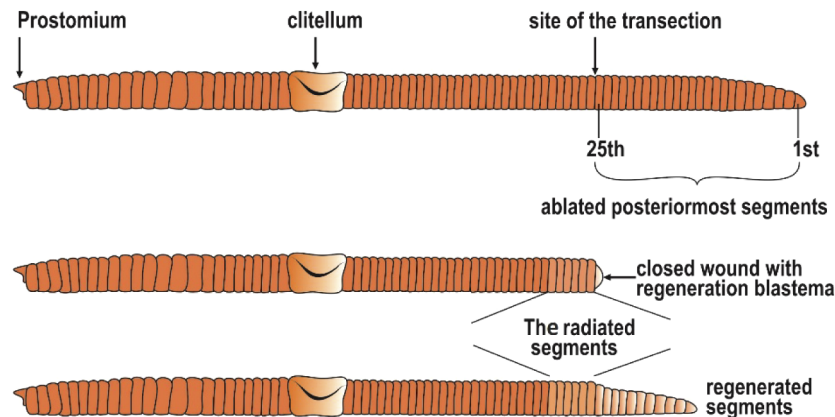


**Fig. 1.** Flowchart of the tail segments removal and regeneration in the earthworm showing the THz radiated body part.

## 2.3. Further handling and experimental treatment of worms

Immediately after the segment ablation, the animals were distributed into three groups, each with 15 specimens, and kept at room temperature (24 °C) in garden compost wetted with tap water. Group C was the control (sham-exposed), group T received purely THz irradiation, and group G was exposed to green light (second harmonic of the infrared laser light). Before the irradiation, worms of all groups were selected from the compost and anesthetized as described above. Then the worms were laid on a glass holder and placed on the exposition field of the equipment (Fig. 2). Four or five of their posteriormost segments were irradiated for 5 minutes at the end of the first postoperative hour. The irradiation was repeated on the first and second postoperative days. The control animals were handled similarly to the irradiated ones (including anesthesia), except the exposition to radiation, and they were kept in a plastic holder at room temperature. Immediately after the treatment, the animals were introduced into the mixture of compost and soil. The number of regenerated segments was counted from the 2<sup>nd</sup> postoperative week to the 4<sup>th</sup> one with a stereomicroscope.

## 2.4. Characteristics of the applied irradiation pulses

### 2.4.1. THz pulses

The irradiation setup is shown in Fig. 2. For THz irradiation, the components within the green box were removed from the setup. Single-cycle THz pulses were generated by optical rectification of short infrared laser pulses in LiNbO<sub>3</sub> (LN) crystal using the tilted-pulse-front technique [27],

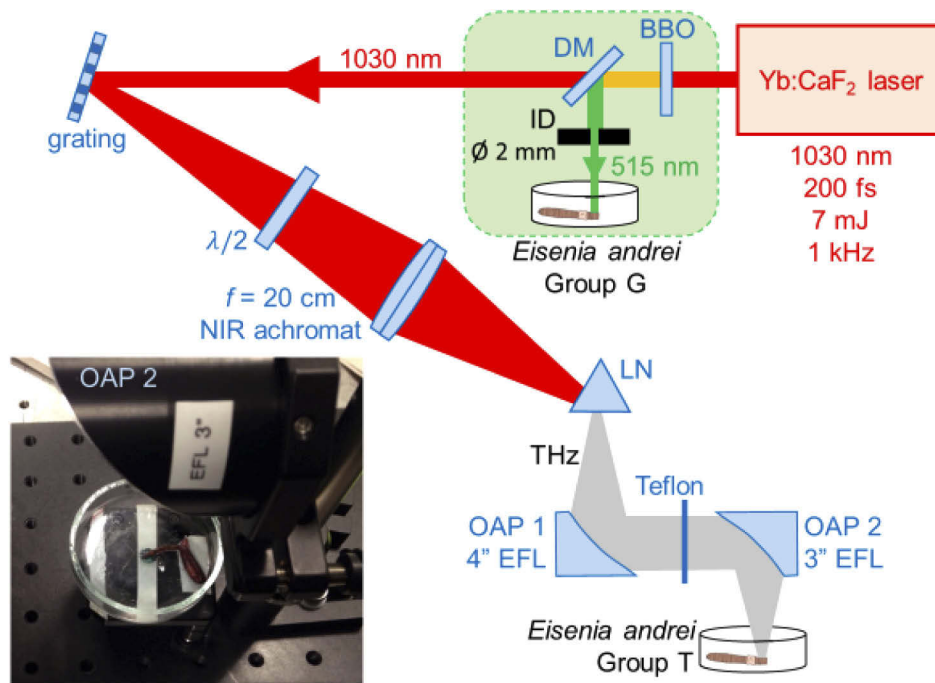


**Fig. 2.** Scheme of the irradiation setup. The *E. andrei* specimens of Group G were placed into the green laser beam. The specimens of Group T were placed into the focus of the THz beam. In this case the components within the green box were removed from the setup. DM: dichroic mirror,  $\lambda/2$ : half-wave retardation plate, OAP: off-axis parabolic mirror, EFL: effective focal length. The bottom left inset shows a photograph of an anaesthetized earthworm at the THz irradiation position.

as shown in Fig. 2. The infrared pump pulses of 1030 nm central wavelength, 200 fs pulse duration, and up to 7 mJ energy were delivered by an Yb:CaF<sub>2</sub> regenerative amplifier at 1 kHz repetition rate. The THz source and its characterization are described in more detail in an earlier study [28]. Briefly, the laser pulse was diffracted off a grating to introduce a pulse-front tilt and imaged from the grating into the LN prism. The generated THz pulses leaving the prism were collimated and focused onto the sample by a pair of off-axis parabolic mirrors with effective focal lengths of 4 and 3 inches (Fig. 2). A Teflon filter between the two parabolic mirrors was used to stop any possible scattered or transmitted optical radiation to reach the sample.

The THz intensity distribution in the focus was measured by a pyroelectric camera (Ophir, model Pyrocam IV). The diameters of the slightly elliptical focal spot were  $2w_x \times 2w_y = 2.14 \text{ mm} \times 2.54 \text{ mm}$  [full widths at  $1/e^2$  of the peak intensity, Fig. 3(a)]. The waveform of the THz pulses was measured by electro-optic sampling and exhibits a single oscillation cycle [Fig. 3(b)]. The measured THz pulse energy ( $W = 5.0 \mu\text{J}$ ), the focal spot size, and the waveform were used to calibrate the peak electric field strength being about  $E_0 = 293 \text{ kV/cm}$  at the beam center. The corresponding peak fluence was  $F_0 = W/(w_x w_y \pi/2) = 234 \mu\text{J/cm}^2$  (assuming Gaussian intensity distribution) and the peak instantaneous intensity  $I_0 = \epsilon_0 c E_0^2 = 229 \text{ MW/cm}^2$ . Here,  $\epsilon_0$  is the permittivity of free space and  $c$  is the speed of light in vacuum. Fourier transformation of the temporal waveform gives the amplitude spectrum  $A(\nu)$  [inset in Fig. 3(b)]. A mean frequency of  $\bar{\nu} = 0.30 \text{ THz}$  was calculated from the spectral intensity  $A^2(\nu)$  according to  $\bar{\nu} = \int_0^\infty \nu A^2(\nu) d\nu / \int_0^\infty A^2(\nu) d\nu$ . This frequency corresponds to an oscillation cycle of  $1/\bar{\nu} = 3.3 \text{ ps}$

(the approximate pulse duration of the single-cycle waveform). The average intensity over the oscillation cycle was  $\bar{I} = F_0 \bar{v} = 70 \text{ MW/cm}^2$  at the beam center.

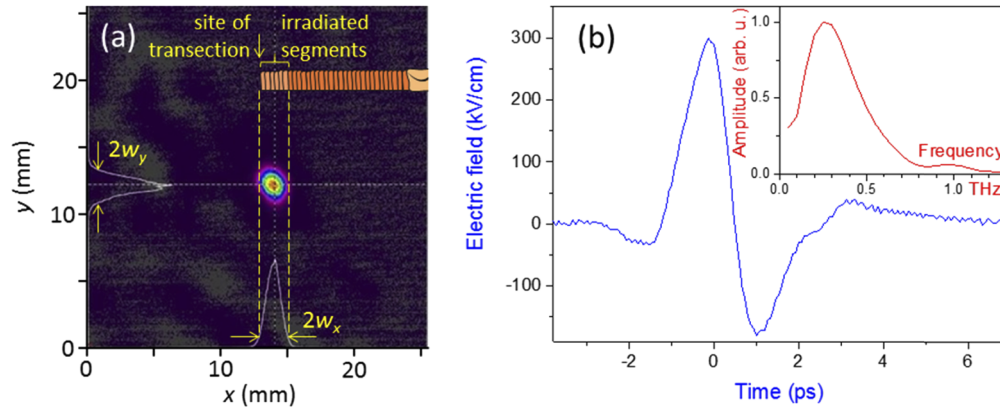


**Fig. 3.** (a) Image of the THz beam spot at the sample location. The inset in the top right shows in side view the nominal position of the *Eisenia andrei* sample along the  $x$  direction. (b) Measured temporal dependence of the THz electric field. The inset shows the amplitude spectrum calculated by Fourier transformation of the waveform.

Special care was taken to precisely determine the beam location in the focal plane and to position the ablated tail part of the animals with the highest possible accuracy relative to the beam. The uncertainty in the animal positioning was about  $\pm 0.5 \text{ mm}$ , giving an estimated uncertainty in the effective sample irradiation of about 15%. This value was obtained by integrating the two-dimensional Gaussian intensity distribution for a sample animal displaced by  $\pm 0.5 \text{ mm}$  from the nominal position, where the site of transection was at  $1/e^2$  of the peak intensity [inset in Fig. 3(a), see also Section 2.3]. Because the root-mean-square energy fluctuation of the THz pulses was about 1%, the main source of uncertainty in the irradiation level was the uncertainty in animal positioning. Similar was the case with the green light irradiation (see Section 2.4.2).

#### 2.4.2. Green light

Group G, with 15 amputated *E. andrei* earthworms, was exposed to green light. This was produced by phase-matched second-harmonic generation of the infrared laser pulses in a BBO crystal (Fig. 2). The beam diameter was adjusted by an iris diaphragm to 2 mm and the pulse energy was set to  $5 \mu\text{J}$  (the same as that of the THz pulses). A dichroic mirror, transmitting the infrared and reflecting the green, was used to separate the two wavelengths.

#### 2.5. Regeneration blastema formation and kinetics of segment regeneration

The wound closure, regeneration blastema, and renewing segment formation was studied with both anatomical and histological methods on the sixth postoperative hour, and further on weekly till the fourth postoperative week. The earliest unambiguous identification of the regenerating segments was possible based on the strip-like accumulation of yellow colored coelomocytes in the forming coelomic sacs on the first postoperative week. Later on, segment boundaries were already clearly seen because of the segmental organization of the circular muscles of the body wall (Fig. 4). Because of the triplicate repetition of the experiments the average segment number was calculated based on the investigation of  $3 \times 15$  animals from each group.



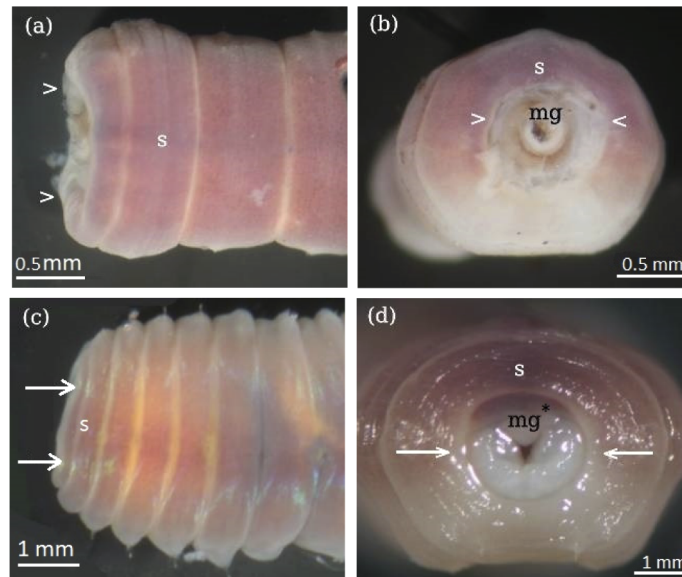


**Fig. 4.** Anatomical characteristics of the segments in freshly operated animals (a,b), and in the sixth postoperative hour (c,d). Note that in the freshly cut segment, a quick contraction of the body wall can be seen, whereas, in the 6<sup>th</sup> postoperative hour, the fusion of the body wall and the midgut can be observed, forming a new internal opening. Abbreviations: mg - midgut, mg\*: midgut is covered by thin layer of blast cells, s: segment, arrowheads label contracting body wall in (a,b), the arrow lines label the fusion of the tissues of body wall and midgut (c,d).

## 2.6. Histological investigations

The time course of the regeneration was investigated on the 6<sup>th</sup> postoperative hours and on weekly from the 1<sup>st</sup> to the 4<sup>th</sup> postoperative periods. From anaesthetized animals (5 from each group) the regenerating body parts with 3 or 4 original segments were dissected and fixed in freshly prepared formalin-acetic acid solution (6 ml 38% formalin, 1 ml cc. acetic acid, and 18 ml distilled water), developed in our laboratory, for 72 hours at room temperature. Prolonged fixation for 2 weeks did not influence the staining properties of the sections. The fixed samples were washed and embedded into Paraplast Xtra (Merck Group, Hungary) as usual. Serial sections with 10  $\mu\text{m}$  were cut with a rotary microtome and attached to gelatin coated slides and stained with Mayer's hematoxylin and eosin according to the conventional microtechnical protocols [29]. After dehydration and clearing with xylene, sections were coverslipped by DPX mountant, then investigated by a Nikon Optiphot-2 photomicroscope.

## 2.7. Calculation of the mitotic index (MI) characteristic for distinct body parts

The number of interphase nuclei and mitotic figures (pro-, meta-, ana-, and telophase) was counted in 10 consecutive high power fields (400-fold magnification) of distinct parts of both original and regenerating segments of group C (sham-exposed), group G, and T animals, respectively. The mitotic cells were identified based on their cytological characteristics. In nuclear aggregates, the presence of the definite filamentous projections of chromatin (chromosomes) was observed. The chromosome clumps of both ana- and telophase were counted as one mitotic figure. For calculation of the MI, the following formula was used:

$$\text{MI} = \frac{\text{P} + \text{M} + \text{A} + \text{T}}{\text{N}} \cdot 100\%. \quad (1)$$

Here,  $(P + M + A + T)$  is the sum of all cells in mitotic phase as prophase, metaphase, anaphase, and telophase, respectively, and  $N$  is the total number of cells counted. Apoptotic cells (having strongly condensed chromatin and cytoplasm) were clearly distinguished and they were not counted.

### 2.8. Statistics

Statistical analysis was performed with a computerized statistical package (SPSS). Results were presented as mean and all error bars represented the standard error of the mean. The effect of treatments was analyzed statistically by Student's t-test (means: paired, two-sample equal variance)  $p < 0.01$ , and  $p < 0.05$  were denoted as statistically significant.

## 3. Results

### 3.1. Wound closure and formation of the regeneration blastema

Immediately after the body transection, the body wall muscles contracted and tended to the midgut forming a transient barrier to prevent the loss of the coelomic fluid and the blood. On the first postoperative day, the body wall tissues closely attached to the midgut, and a small circular regeneration blastema (cicatrix) formed between the body wall and midgut tissues (Fig. 4). The histological observations revealed that intense dedifferentiation of the epithelial and muscle layers of both the body wall and midgut contributed to the formation of scar tissues consisting mainly of dedifferentiated epithelial and muscle cells, however, few coelomocytes were also dispersed in it (not shown).

No difference was found in the kinetics of the wound closure and histological organization of the regeneration blastema between the control and the irradiated groups. The formation of the regeneration blastema, from which new segments arose, started close to the cut stump of the ventral nerve cord, where small basophil cells with high nucleus-cytoplasm ratio concentrated, which were identified as mesodermal stem cells (neoblasts), thought to be key players in regeneration (not shown).

### 3.2. Kinetics of segment regeneration

The first renewed segments were clearly seen by a stereomicroscope after the first postoperative week [Figs. 5(a), 5(c)], however their size extremely varied from animal to animal, and their number could not be definitely determined. In contrast to the first postoperative week, from the second week on, each regenerating segment was unambiguously identifiable. Therefore, the kinetics of segment regeneration of distinct experimental groups was compared from this point of time.

A huge difference in the regenerated segment number was found between the distinct groups of the experimental animals. Whereas THz pulses significantly stimulated the formation of the new segments, the green light did not have any influence on segment regeneration, indicated by nearly equal segment numbers to those in the control group (Fig. 6). The trend of the segment regeneration was the same on the third and fourth postoperative weeks, with about three times higher regenerated segment numbers in the THz-exposed animals than in green-exposed and control ones.

### 3.3. Histological characteristics of the regenerated segments in control and THz-exposed earthworms in the second postoperative week

Since renewing segments were unambiguously distinguishable on the second postoperative week and the intense segment formation also started at this time, the histological observations were focused on the 2<sup>nd</sup> week of the regeneration. The basic histological characteristics of the regenerated segments in group C (sham-exposed), group G (green light exposed) and T (THz

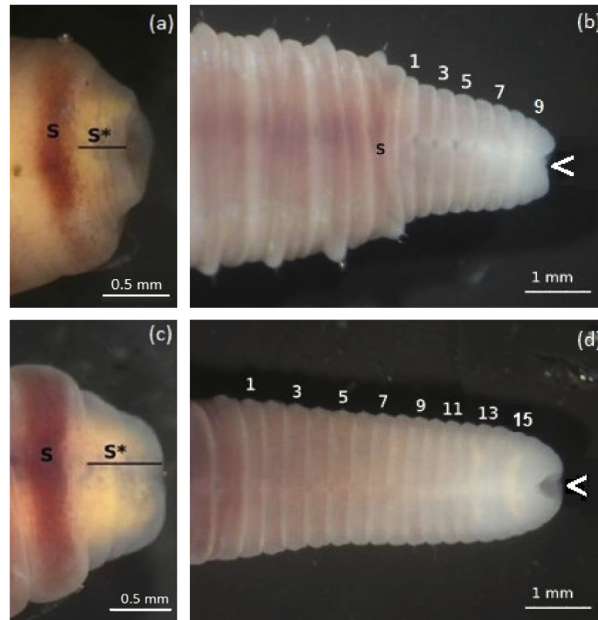


**Fig. 5.** Comparison of the regenerated segment number of the control group (a,b) and THz-irradiated group (c,d) worms on the 7<sup>th</sup> (a,c) and on the 21<sup>st</sup> (b,d) postoperative day. Abbreviations: s: operated segment, s\*: regenerating segments on the first postoperative week, Arabic numerals: regenerating segments on the third postoperative week, arrowheads: anus.

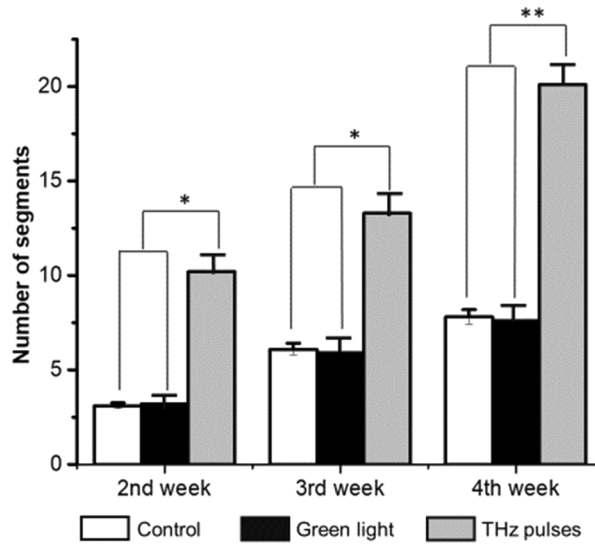


**Fig. 6.** Kinetics of the segment regeneration in control (sham-exposed) and green light or THz irradiated *E. andrei* earthworms. Data represent mean  $\pm$  SEM (n=45, \*, p < 0.05, \*\*, p < 0.01).



exposed) worms were the same. Namely, the ventral part of the regenerated segments, connected to the old segment containing the ventral nerve cord (VNC), was significantly better differentiated than their dorsal parts. The formation of renewing segments could easily be identified based on the differentiating segment boundaries (dissepiments), whereas in renewing dorsal parts no segment differentiation was seen. The differentiation of the ventral nerve cord ganglia was faster than the differentiation of the body wall and the alimentary canal tissues.

Whereas group C and G animals showed the same histological characteristics, there were some marked histological alterations in THz-exposed specimens on the 14<sup>th</sup> postoperative day. In both the group C and G animals, the differentiation of the renewing body wall and VNC ganglia was on a smaller scale than in the T group because not only thinner but also less differentiated VNC ganglia and body wall were characteristic of the group C and G worms [ Figs. 7(a), 7(b)]. In about 60% of THz-exposed worms, marked development of the blood vessels was seen in the regenerating segments, and in adjacent tissues of the blood capillaries, a high number of mitotic cells was located while in the residual ones advanced formation of the blood vessels, extension, and differentiation of various cells could be seen. No similar extension of blood vessels was characteristic of group C and G specimens on the 14<sup>th</sup> postoperative day [Figs. 7(c)–7(e)].

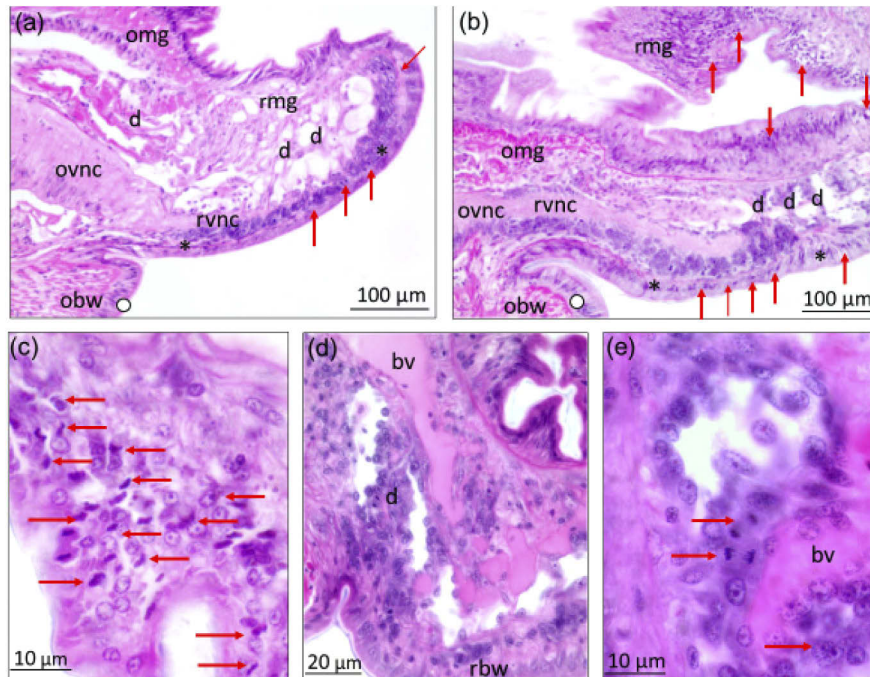


**Fig. 7.** Histological characteristics of the regenerated segments of control (a), and THz-irradiated earthworms (b-e) on the 14<sup>th</sup> postoperative day. Since group G animals are characterized by the same histological alterations than group C ones their sections are not presented in the figure. Abbreviations: ovnc: old ventral nerve cord, rvnc: regenerated ventral nerve cord, obw: old body wall, rbw: regenerated body wall, d: dissepiment, omg: old midgut muscular tissue, rmg: regenerated midgut muscular tissue, bv: blood vessel, arrows: mitotic cells, circles: old epithelial body layer, stars: new epithelial layer.

Comparing the mitotic index of the distinct body parts of experimental animals marked results were collected from the specimens of groups of C, G, and T on the 14<sup>th</sup> postoperative day. Animals of groups of C and G were characterized by a higher MI (0.01) of all renewing structures (body wall and VNC ganglia) than of old ones (MI = 0.002). In specimens of group T, the MI of

all newly formed organs proved to be significantly higher than in groups of C and G ones. For example, the MI of the regenerating VNC ganglia was 0.1, showing intense cell proliferation in these structures. Nearby the newly formed ganglia, several mitotic cells were located in the body wall, alimentary canal, and dissepiments (Figs. 7(d), 7(e)). This conspicuous histological alteration was only found in about 40% of THz-exposed animals at the investigated period, while in others more advanced differentiation of tissues was observed. The smaller, less differentiated regenerating dorsal body parts, which was directly exposed to THz pulses, contained markedly higher number of mitotic figures (MI = 0.2) than the ventral ones (MI = 0.1), characterized by more extended and developed tissues and organs [Fig. 7(c)].

#### 4. Discussion

The influence of electromagnetic waves on morphological and physiological changes of distinct cells and tissues of various species was in the focus of several experiments. Based on their results Hamblin [30] concluded that probably “all life forms respond to light”. Electromagnetic waves can be ionizing and therefore harmful for cells and tissues, damaging the organisms.

In contrast, nonionizing electromagnetic waves (having small photon energy) can trigger photochemical changes within cells in which photon receptive cell organelles and molecules are located. Romanenko et al. reviewed experimental results on the effect of electromagnetic waves on biomolecules and cells and inferred that electromagnetic fields could affect the activity in cell membranes (sodium versus potassium ion conductivities and other non-selective cation channels) [31], membrane potential, and even the cell cycle. They also suggested that THz waves do not cause tissue damage because they do not have enough energy for photoionization. Moreover, THz photon energies are in the energy range of hydrogen bonds, can cause charge transfer reactions and van der Waals interactions, meaning that even simple molecules absorb THz. However, at the same time, an *in vitro* experiment suggested that intense THz radiation causes biological hazard [32]. It was found in an *in vivo* experiment that the skin wound closure of the mice was significantly delayed by repeated femtosecond-THz pulse irradiation (energy up to 30  $\mu$ J, frequencies up to 2.5 THz, duration 1 hour) indicating that THz could have disadvantageous effects on biological systems [14]. The discrepancies between the published experimental results can be the consequence of the application of distinct, non-standardized biological models and various experimental protocols.

The aim of this study was to investigate the effects of high-intensity THz pulses on the standardized posterior segment regeneration of the earthworm *E. andrei*. Segment regeneration has certain discrete phases, constituting the post-extirpation repairing process, like (i) sealing the slotted segment via rapid muscular contraction, preventing loss of body fluids and microbial attacks, (ii) stimulation of tissue dedifferentiation and migration of mesodermal stem cells (neoblasts), scattered over all segments, to the site of the injury resulting in (iii) the formation of the regeneration blastema [33,34]. Both dedifferentiated cells and neoblasts produce a high number of new cells by proliferation through cell division (mitosis) and their differentiation creates the new tissues and organs of the regenerating segments. In segment regeneration, there are several regulators as key players. Some of them mediate dedifferentiation, migration, and proliferation of various cells, others the differentiation of new tissues, organs, and segments, while certain regulators stop the cell division and differentiation terminating the segment formation of the abnormal cells and structures [35,36].

No difference in the first step (wound closure) of the regeneration was found between the irradiated and control animals: in all three groups, the wound was closed at the sixth postoperative hour with the fusion of the body wall and alimentary canal tissues (Fig. 4). However, on the first postoperative week, more advanced development of the regeneration blastema was observed in THz-irradiated earthworms (Fig. 5). The regeneration blastema consists of dedifferentiated tissue cells and some migrating neoblasts [32]. Cell proliferation depends on a dynamic realignment of

actin filaments in both cyto- and nucleoplasm [23]. An *in vitro* experiment showed that THz radiation modulated actin filament polymerization from soluted (globular) actin suggesting that the *in vivo* actin polymerization, mediated by any influence, contributes to the regulation of some significant processes, like gene expression, cell motility, and growth [37]. Yamazaki et al. reported that THz radiation has negligible effects on deep tissues of the human body due to strong absorption by water molecules, however, the energy of THz pulses, possibly as a shockwave, has transmitted a millimeter thick tissue in the aqueous solution and demolished actin filaments [38]. They also showed that the viability of the cell was not affected under the exposure of THz pulses.

A recent finding suggests that the blastema growth in Planarians is mediated by infrared, blue, and green light. It was found that green light exposure reduced the growth of the head blastema, while red light exposure stimulated its growth. No significant difference was found in the proliferation of neoblasts under green or red light exposure which suggests that these expositions influence the migration of the neoblasts to the amputation site [39]. In our experiments, green light did not affect segment regeneration from which we propose that in earthworms the formation of the regeneration blastema is determined by a more complex process than in Planarians and cell dedifferentiation and redifferentiation are more important in earthworm regeneration.

In our experiments, the applied THz pulses significantly stimulated the segment regeneration: irradiated animals renewed about three times higher number of segments than control specimens. The maintenance of the segments' structure and functions needs a well-controlled balance between the continuous cell proliferation and differentiation throughout the life of an animal [40]. This balance is perturbed after any injury of the body (e.g. wound) and imbalance is a characteristic feature of the regenerating tissues. In the regenerating rat liver hepatocytes were characterized by an elevated mitotic activity but mitotic cells appeared at various points of time during the regeneration suggesting that there were unsynchronized mitotic waves during the regeneration [41]. A similar situation can appear in earthworms as well. The experimental animals could have distinct physiological states, so after the segment ablation, the cell proliferation could be started at various times. Therefore, distinct timing of the cell proliferation and differentiation could be seen in the experimental animals resulting that some specimens were characterized by intense cell proliferation while others with intense cell growing and differentiation at a fixed time of the regeneration. Nevertheless, the presented histological alterations (e.g. accumulation of mitotic cells in the epithelial layers, extension of blood vessels) were found in THz-irradiated specimens exclusively and were not seen in any animals of groups C and G.

No malformation in segment organization was found. What is more, some advantageous alterations, like more extended primordium of the VNC and more intense segment formation and advanced blood vessel development, were observed [Fig. 7(c)]. It is evident that the formation of the higher number of the renewed segments needs a lot of more new cells and their differentiation for tissue cells. New cells are produced by mitosis when semiconservative replication of the DNA and synthesis of some regulatory proteins which mediate cell divisions are carried out [37]. The effect of THz radiation on DNA molecules and cell proliferation is a debated question. In the human skin tissue model, the exposure of various cells to THz pulse at energies of 1.0  $\mu\text{J}$  and 0.1  $\mu\text{J}$  for 10 minutes resulted in DNA damage and subsequent cell growth [42]. Exposure of artificial human skin tissue to intense THz pulses caused increased expression levels of numerous genes associated with non-melanoma skin cancers, psoriasis, and atopic dermatitis. However, changes in the expression of nearly half of the epidermal differentiation complex (EDC) members were also found suggesting that the THz-induced changes in transcription levels were opposite to disease-related changes [43].

The effect of long-term (6 hours) THz irradiation on human cells was investigated by Zhao et al. [44]. It was found that long-term THz irradiation generated a specific change in gene expression resulting in abnormal chromosome number (aneuploidy) in some daughter cells. Intense exposition of cells to THz pulses induced the expression of both tumor-suppressing and

oncogenic genes in human skin cells found by Hough et al. [45]. On the other hand, THz radiation at 0.38 THz and 2.52 THz did not lead to DNA damage in skin cells *in vitro*. Furthermore, no chromosomal damage was detected and quantified cell proliferation was found to be unaffected by the exposure [46]. A recent study suggests that THz wave exposure with very low intensity does not affect cell proliferation or cell growth rates [11].

At present, there is only weak evidence that THz pulses can influence cell proliferation (mitosis) and differentiation. The effect of broadband THz radiation on mammalian (mouse) stem cells was investigated by Bock et al. [13]. They found that radiation-induced specific changes in cellular functions were closely related to DNA-directed gene transcription. Surveying of gene expression, it was found that 11% of genes responded to the applied THz irradiation, either upregulated or downregulated, and based on the accelerated cell differentiation they concluded that THz radiation could be a potential tool for cellular reprogramming [13]. The segment regeneration needs both intense cell proliferation and differentiation. However, details of the regulation are not known yet. We found that the applied THz pulses stimulated the formation of a high number of new segments. Based on this, we suppose that THz pulses influence the activity of various biomolecules like proteins, DNA, and RNA due to the conformational changes as was reported by Lee [47].

Investigating the effect of THz pulses on human induced pluripotent stem cells THz pulses could alter the expression of certain genes and they were driven by zinc-finger transcription factors and it was supposed that the local intracellular concentration of metal ions, such as  $Zn^{2+}$ , was changed by the effective electrical force of the applied THz pulse. However, there is a large phylogenetic distance between humans and earthworms, the zinc-finger transcription factors are probably present in the latter one as well, as it has been found by Tachizaki et al. [48]. A putative zinc-finger protein as a gene activator was identified in a lumbricid earthworm [49], therefore there is a possibility that similar molecular and cellular processes are stimulated by THz pulses in earthworms similarly to human cells.

Currently, segment regeneration is a largely unknown process characterized by some enigmatic cytological and histological alterations. However, there is some experimental evidence that anatomical, physiological, and cellular factors influence the kinetics of segment regeneration. The best documented neural dependence of regeneration was promulgated by Morgan [16] for the first time and supported by some experimental evidences later. The formation of the regeneration blastema is started at the cut end of the VNC from which neural processes outgrow and spread amongst tissue cells [50]. Discharged neural substances, certain neurotransmitters, and neurohormones stimulate the segment regeneration by regulating the functioning of various tissues [17,18]. Tan et al. found that the primary cultured neurons responded to the THz radiation and the induced biological effects were positively correlated with the exposure time of the THz waves [12]. The marked decrease in the neurotransmitter content (glutamate) of some neurons were detected as well. An *in vivo* THz radiation can generate a similar neurotransmitter release from neurons stimulating the formation of the regeneration blastema and differentiation of its cells. Although, Borovkova et al. showed a dose-dependent cytotoxic effect of THz radiation on glial cells [32], in our experiments no significant number of necrotic or apoptotic cells was found in any tissues. In contrast to the effect of repeated femtosecond-THz radiation (energy up to 30  $\mu$ J, frequencies up to 2.5 THz, duration 1 hour) applied in a wound-healing experiment [14], the used THz exposure (energy 5  $\mu$ J, 0.3 THz frequency, irradiation time 5 min) in our experiments has an advantageous effect on wound healing and it has been experimentally proven on tissue and organ regeneration of earthworms. This strongly suggests that the parameters of THz exposure (energy, frequency, irradiation time) can significantly influence its biological effects.

Segment regeneration of earthworms can be a useful model to investigate the effect of various factors on the phenotypic changes (both anatomical and physiological) at the organism level.



Certain physical effects, like temperature, modify the kinetics of segment regeneration e.g. the long-term (several days) cooling of the experimental animals after the surgical intervention resulted in lower segment regeneration in various earthworm species [51]. Moment investigated the effect of the ionizing X-ray irradiation on the five posteriormost segments located afore the transection and found that its effect on the regeneration was dose-dependent. Only a high dose of X-ray radiation (from 20,000 R) blocked the formation of new tissues and organs [52]. Based on the observations mentioned above, we suppose that the kinetics of segment formation is an effective indicator of both inhibitory and stimulatory effects of various factors. Therefore, it can be used as a model at the organism level to investigate the biological effects of distinct electromagnetic waves.

## 5. Conclusion

The presented results show that the posterior segment regeneration of earthworms is a suitable model to investigate the biological effects of THz pulses at the organism level and suggest that there are certain interactions between THz radiation and biomolecules (proteins, nucleic acids, etc.), cells, and tissues. The applied intense THz pulses significantly stimulated the segment regeneration. No abnormal tissue or segment development occurred in the experimental animals during the four-week-long experiments. Based on these findings, we can propose that the applied THz radiation has beneficial effects on both cell proliferation and differentiation, and on tissue development. Further *in vivo* experiments are needed to ascertain the exact influence of THz radiation on cell proliferation and differentiation. The present study can contribute to the improvement of biomedical application of THz pulses.

**Funding.** National Research, Development and Innovation Office (2018-1.2.1-NKP-2018-00009, 2018-2.1.5-NEMZ-2018-00003); Eurostars (E 12576 HABRIA); European Social Fund (17886 4/2018/FEKUTSTRAT, EFOP-3.6.2-16-2017-00005).

**Disclosures.** The authors declare no conflicts of interest.

## References

1. L. Zhao, Y.-H. Hao, and R.-Y. Peng, "Advances in the biological effects of terahertz wave radiation," *Mil. Med. Res.* **1**(1), 1–4 (2014).
2. G. J. Wilmlink, B. D. Rivest, C. C. Roth, B. L. Ibey, J. A. Payne, L. X. Cundin, J. E. Grundt, X. Peralta, D. G. Mixon, and W. P. Roach, "In vitro investigation of the biological effects associated with human dermal fibroblasts exposed to 2.52 THz radiation," *Lasers Surg. Med.* **43**(2), 152–163 (2011).
3. G. J. Wilmlink, B. D. Rivest, B. L. Ibey, C. L. Roth, J. Bernhard, and W. P. Roach, "Quantitative investigation of the bioeffects associated with terahertz radiation," *Opt. Interact. with Tissues Cells XXI* 7562, 75620L (2010).
4. J. S. Olshevskaya, A. S. Ratushnyak, A. K. Petrov, A. S. Kozlov, and T. A. Zapara, "Effect of terahertz electromagnetic waves on neurons systems," *Int. Conf. Comput. Technol. Electr. Electron. Eng.* 210–211 (2008).
5. M. R. Scarfi, M. Romanò, R. D. I. Pietro, O. Zeni, and A. Doria, "THz Exposure of Whole Blood for the Study of Biological Effects on Human Lymphocytes," *J. Biol. Phys.* **29**(2/3), 171–176 (2003).
6. O. Zeni, G. P. Gallerano, A. Perrotta, M. Romanò, A. Sannino, M. Sarti, M. D'Arienzo, A. Doria, E. Giovenale, A. Lai, G. Messina, and M. R. Scarfi, "Cytogenetic observations in human peripheral blood leukocytes following in vitro exposure to THz radiation: A pilot study," *Health Phys.* **92**(4), 349–357 (2007).
7. A. Korenstein-Ilan, A. Barbul, P. Hasin, A. Eliran, A. Gover, and R. Korenstein, "Terahertz radiation increases genomic instability in human lymphocytes," *Radiat. Res.* **170**(2), 224–234 (2008).
8. N. Bourne, R. H. Clothier, M. D'Arienzo, and P. Harrison, "The effects of terahertz radiation on human keratinocyte primary cultures and neural cell cultures," *ATLA, Altern. Lab. Anim.* **36**(6), 667–684 (2008).
9. R. H. Clothier and N. Bourne, "Effects of THz exposure on human primary keratinocyte differentiation and viability," *J. Biol. Phys.* **29**(2/3), 179–185 (2003).
10. R. Williams, A. Schofield, G. Holder, J. Downes, D. Edgar, P. Harrison, M. Siggel-King, M. Surman, D. Dunning, S. Hill, D. Holder, F. Jackson, J. Jones, J. McKenzie, Y. Saveliev, N. Thomsen, P. Williams, and P. Weightman, "The influence of high intensity terahertz radiation on mammalian cell adhesion, proliferation and differentiation," *Phys. Med. Biol.* **58**(2), 373–391 (2013).
11. N. Yaekashiwa, H. Yoshida, S. Otsuki, S. Hayashi, and K. Kawase, "Verification of Non-thermal Effects of 0.3–0.6 THz-Waves on Human Cultured Cells," *Photonics* **6**(1), 33 (2019).



12. S. Z. Tan, P. C. Tan, L. Q. Luo, Y. L. Chi, Z. L. Yang, X. L. Zhao, L. Zhao, J. Dong, J. Zhang, B. W. Yao, X. P. Xu, G. Tian, J. K. Chen, H. Wang, and R. Y. Peng, "Exposure Effects of Terahertz Waves on Primary Neurons and Neuron-like Cells Under Nonthermal Conditions," *Biomed. Environ. Sci.* **32**(10), 739–754 (2019).
13. J. Bock, Y. Fukuyo, S. Kang, M. Lisa Phipps, L. B. Alexandrov, K. O. Rasmussen, A. R. Bishop, E. D. Rosen, J. S. Martinez, H. T. Chen, G. Rodriguez, B. S. Alexandrov, and A. Usheva, "Mammalian stem cells reprogramming in response to terahertz radiation," *PLoS One* **5**(12), 8–13 (2010).
14. K. T. Kim, J. Park, S. J. Jo, S. Jung, O. S. Kwon, G. P. Gallerano, W. Y. Park, and G. S. Park, "High-Power Femtosecond-Terahertz Pulse Induces a Wound Response in Mouse Skin," *Sci. Rep.* **3**(1), 2296 (2013).
15. E. Varhalmi, I. Somogyi, G. Kiszler, J. Nemeth, D. Reglodi, A. Lubics, P. Kiss, A. Tamas, E. Pollak, and L. Molnar, "Expression of PACAP-like compounds during the caudal regeneration of the earthworm *Eisenia fetida*," *J. Mol. Neurosci.* **36**(1-3), 166–174 (2008).
16. T. H. Morgan, "Experimental studies of the regeneration of *Planaria maculata*," *Dev. Genes Evol.* **7**(2-3), 364–397 (1898).
17. I. Somogyi, A. Boros, P. Engelmann, E. Varhalmi, J. Nemeth, A. Lubics, A. Tamas, P. Kiss, D. Reglodi, E. Pollak, and L. Molnar, "Pituitary adenylate cyclase-activating polypeptide-like compounds could modulate the activity of coelomocytes in the earthworm," *Ann. N. Y. Acad. Sci.* **1163**(1), 521–523 (2009).
18. L. Molnar, E. Pollak, Z. Skopek, E. Gutt, J. Kruk, A. J. Morgan, and B. Plytycz, "Immune system participates in brain regeneration and restoration of reproduction in the earthworm *Dendrobaena veneta*," *Dev. Comp. Immunol.* **52**(2), 269–279 (2015).
19. V. Takacs, L. Molnar, B. Klimek, A. Gałuszka, A. J. Morgan, and B. Plytycz, "Exposure of *Eisenia andrei* (Oligochaeta; Lumbricidae) to cadmium polluted soil inhibits earthworm maturation and reproduction but not restoration of experimentally depleted coelomocytes or regeneration of amputated segments," *Folia Biol.* **64**(4), 275–284 (2016).
20. K. Hamana, H. Hamana, and T. Shinozawa, "Alterations in polyamine levels of nematode, earthworm, leech and planarian during regeneration, temperature and osmotic stresses," *Comp. Biochem. Physiol., Part B: Biochem. Mol. Biol.* **111**(1), 91–97 (1995).
21. A. Amaroli, D. Agas, F. Laus, V. Cuteri, R. Hanna, M. G. Sabbieti, and S. Benedicenti, "The effects of photobiomodulation of 808 nm diode laser therapy at higher fluence on the in vitro osteogenic differentiation of bone marrow stromal cells," *Front. Physiol.* **9**(2), 1–11 (2018).
22. A. E. Bely, "Early events in annelid regeneration: a cellular perspective," *Integr. Comp. Biol.* **54**(4), 688–699 (2014).
23. E. E. Zattara, K. W. Turlington, and A. E. Bely, "Long-term time-lapse live imaging reveals extensive cell migration during annelid regeneration," *BMC Dev. Biol.* **16**(1), 6–21 (2016).
24. B. D. Özpölat and A. E. Bely, "Developmental and molecular biology of annelid regeneration: a comparative review of recent studies," *Curr. Opin. Genet. Dev.* **40**, 144–153 (2016).
25. L. Molnár, P. Engelmann, I. Somogyi, L. L. Mácsik, and E. Pollák, "Cold-stress induced formation of calcium and phosphorous rich chloragocyte granules (chloragosomes) in the earthworm *Eisenia fetida*," *Comp. Biochem. Physiol., Part A: Mol. Integr. Physiol.* **163**(2), 199–209 (2012).
26. P. D. N. Hebert, A. Cywinska, S. L. Ball, and J. R. DeWaard, "Biological identifications through DNA barcodes," *Proc. R. Soc. London, Ser. B* **270**(1512), 313–321 (2003).
27. J. Hebling, G. Almasi, I. Kozma, and J. Kuhl, "Velocity matching by pulse front tilting for large area THz-pulse generation," *Opt. Express* **10**(21), 1161 (2002).
28. C. Lombosi, G. Polónyi, M. Mechler, Z. Ollmann, J. Hebling, and J. A. Fülöp, "Nonlinear distortion of intense THz beams," *New J. Phys.* **17**(8), 083041 (2015).
29. A. S. John D. Bancroft, [*Theory and practice of histological techniques*] (1990).
30. M. R. Hamblin, "Mechanisms and Mitochondrial Redox Signaling in Photobiomodulation," *Photochem. Photobiol.* **94**(2), 199–212 (2018).
31. S. Romanenko, R. Begley, A. R. Harvey, L. Hool, and V. P. Wallace, "The interaction between electromagnetic fields at megahertz, gigahertz and terahertz frequencies with cells, tissues and organisms: Risks and potential," *J. R. Soc., Interface* **14**(137), 20170585 (2017).
32. M. Borovkova, M. Serebriakova, V. Fedorov, E. Sedykh, V. Vaks, A. Lichutin, A. Salnikova, and M. Khodzitsky, "Investigation of terahertz radiation influence on rat glial cells," *Biomed. Opt. Express* **8**(1), 273 (2017).
33. E. E. Zattara and A. E. Bely, "Evolution of a novel developmental trajectory: Fission is distinct from regeneration in the annelid *Pristina leidyi*," *Evol. Dev.* **13**(1), 80–95 (2011).
34. M. Weidhase, C. Helm, and C. Bleidorn, "Morphological investigations of posttraumatic regeneration in *Timarete cf. punctata* (Annelida: Cirratulidae)," *Zoological Lett.* **1**(1), 1–16 (2015).
35. H. Herlant-Mewis, "Regeneration in Annelids," *Adv. Morphog.* **4**, 155–215 (1964).
36. M. Mitsushima, K. Aoki, M. Ebisuya, S. Matsumura, T. Yamamoto, M. Matsuda, F. Toyoshima, and E. Nishida, "Revolving movement of a dynamic cluster of actin filaments during mitosis," *J. Cell Biol.* **191**(3), 453–462 (2010).
37. S. Yamazaki, M. Harata, T. Idehara, K. Konagaya, G. Yokoyama, H. Hoshina, and Y. Ogawa, "Actin polymerization is activated by terahertz irradiation," *Sci. Rep.* **8**(1), 1–7 (2018).
38. T. Yamazaki, A. Kirchmair, A. Sato, A. Buqué, M. Rybstein, G. Petroni, N. Bloy, F. Finotello, L. Stafford, E. Navarro Manzano, F. Ayala de la Peña, E. García-Martínez, S. C. Formenti, Z. Trajanoski, and L. Galluzzi, "Mitochondrial DNA drives abscopal responses to radiation that are inhibited by autophagy," *Nat. Immunol.* **21**(10), 1160–1171 (2020).

39. A. M. Ermakov, O. N. Ermakova, A. L. Popov, A. A. Manokhin, and V. K. Ivanov, "Opposite effects of low intensity light of different wavelengths on the planarian regeneration rate," *J. Photochem. Photobiol., B* **202**, 111714 (2020).
40. L. Zhu and A. I. Skoultchi, "Coordinating cell proliferation and differentiation," *Curr. Opin. Genet. Dev.* **11**(1), 91–97 (2001).
41. J. I. Fabrikant, "The kinetics of cellular proliferation in regenerating liver," *J. Cell Biol.* **36**(3), 551–565 (1968).
42. L. V. Titova, A. K. Ayesheshim, A. Golubov, D. Fogen, R. Rodriguez-Juarez, F. A. Hegmann, and O. Kovalchuk, "Intense THz pulses cause H2AX phosphorylation and activate DNA damage response in human skin tissue," *Biomed. Opt. Express* **4**(4), 559 (2013).
43. L. V. Titova, A. K. Ayesheshim, A. Golubov, R. Rodriguez-Juarez, R. Woycicki, F. A. Hegmann, and O. Kovalchuk, "Intense THz pulses down-regulate genes associated with skin cancer and psoriasis: A new therapeutic avenue," *Sci. Rep.* **3**(1), 2363 (2013).
44. J. W. Zhao, M. X. He, L. J. Dong, S. X. Li, L. Y. Liu, S. C. Bu, C. M. Ouyang, P. F. Wang, and L. L. Sun, "Effect of terahertz pulse on gene expression in human eye cells," *Chin. Phys. B* **28**(4), 048703 (2019).
45. C. M. Hough, D. N. Purschke, C. Huang, L. V. Titova, O. Kovalchuk, B. J. Warkentin, and F. A. Hegmann, "Topology-Based Prediction of Pathway Dysregulation Induced by Intense Terahertz Pulses in Human Skin Tissue Models," *J. Infrared, Millimeter, Terahertz Waves* **39**(9), 887–898 (2018).
46. H. Hintzsche, C. Jastrow, B. Heinen, K. Baaske, T. Kleine-Ostmann, M. Schwerdtfeger, M. K. Shakfa, U. Kärst, M. Koch, T. Schrader, and H. Stopper, "Terahertz radiation at 0.380 THz and 2.520 THz does not lead to DNA damage in skin cells in vitro," *Radiat. Res.* **179**(1), 38–45 (2013).
47. Y. S. Lee., [Principles of Terahertz science and technology], Springer (2008).
48. T. Tachizaki, R. Sakaguchi, S. Terada, K.-I. Kamei, and H. Hirori, "Terahertz pulse-altered gene networks in human induced pluripotent stem cells," *Opt. Lett.* **45**(21), 6078 (2020).
49. M. Höckner, R. Dallinger, and S. R. Stürzenbaum, "Metallothionein gene activation in the earthworm (*Lumbricus rubellus*)," *Biochem. Biophys. Res. Commun.* **460**(3), 537–542 (2015).
50. P. W. Reddien and A. Sánchez Alvarado, "Fundamentals of planarian regeneration," *Annu. Rev. Cell Dev. Biol.* **20**(1), 725–757 (2004).
51. G. B. Moment, "The relation of body level, temperature, and nutrition to regenerative growth," *Physiol. Zool.* **26**(2), 108–117 (1953).
52. G. B. Moment, "Recovery and abscopal effects after inhibitory x-irradiation in earthworm regeneration," *J. Exp. Zool.* **181**(1), 33–39 (1972).